Radiology

ORIGINAL RESEARCH • NEURORADIOLOGY

Choroid Plexus Volume and Permeability at Brain MRI within the Alzheimer Disease Clinical Spectrum

Jong Duck Choi, MD • Yeonsil Moon, MD, PhD • Hee-Jin Kim, MD, PhD • Younghee Yim, MD • Subin Lee, PhD • Won-Jin Moon, MD, PhD

From the Departments of Radiology (J.D.C., W.J.M.) and Neurology (Y.M.), Konkuk University Medical Center, Konkuk University School of Medicine, 120-1 Neungdong-ro, Hwayang-dong, Gwangjin-gu, Seoul 05030, Korea; Research Institute of Medical Science, Konkuk University School of Medicine, Seoul, Korea (Y.M., W.J.M.); Department of Neurology, Hanyang University Hospital, Hanyang University School of Medicine, Seoul, Korea (H.J.K.); Department of Radiology, Chung-Ang University Hospital, Chung-Ang University School of Medicine, Seoul, Korea (Y.Y.); and Department of Electrical and Computer Engineering, Seoul National University, Seoul, Korea (S.L.). Received September 25, 2021; revision requested November 11; revision received March 2, 2022; accepted March 18. **Address correspondence to** W.J.M. (email: *mdmoonwj@kuh.ac.kr*).

Supported by the National Research Foundation of Korea (NRF) and funded by the Korean government (Ministry of Science, ICT and Future Planning) (grant 2020R1A2C1102896) and the Korea Health Technology R&D Project through the Korea Health Technology R&D Project via the Korea Health Industry Development Institute, funded by the Ministry of Health and Welfare, Republic of Korea (grant HU21C0222).

Conflicts of interest are listed at the end of this article.

See also the editorial by Chiang in this issue.

Radiology 2022; 000:1–11 • https://doi.org/10.1148/radiol.212400 • Content codes: NR MR

Background: Mounting evidence suggests that the choroid plexus (CP) plays an important role in the pathophysiology of Alzheimer disease (AD), but its imaging profile in cognitive impairment remains unclear.

Purpose: To evaluate CP volume, permeability, and susceptibility by using MRI in patients at various stages of cognitive impairment.

Materials and Methods: This retrospective study evaluated patients with cognitive symptoms who underwent 3.0-T MRI of the brain, including dynamic contrast-enhanced (DCE) imaging and quantitative susceptibility mapping (QSM), between January 2013 and May 2020. CP volume was automatically segmented using three-dimensional T1-weighted sequences; the volume transfer constant (ie, K^{trans}) and fractional plasma volume (ie, V_p) were determined using DCE MRI, and susceptibility was assessed using QSM. The effects of CP volume, expressed as the ratio to intracranial volume, on cognition were evaluated using multivariable linear regression adjusted for age, sex, education, apolipoprotein E ε4 allele status, and volumetric measures.

Results: A total of 532 patients with cognitive symptoms (mean age, 72 years ± 9 [SD]; 388 women) were included: 78 with subjective cognitive impairment (SCI), 158 with early mild cognitive impairment (MCI), 149 with late MCI, and 147 with AD. Among these, 132 patients underwent DCE MRI and QSM. CP volume was greater in patients at more severe stages (ratio of intracranial volume × 10^3: 0.9 ± 0.3 for SCI, 1.0 ± 0.3 for early MCI, 1.1 ± 0.3 for late MCI, and 1.3 ± 0.4 for AD; $P < .001$). Lower K^{trans} ($r = -0.19$; $P = .03$) and V_p ($r = -0.20$; $P = .02$) were negatively associated with CP volume; susceptibility was not ($r = 0.15$; $P = .10$). CP volume was negatively associated with memory ($B = -0.67$; standard error of the mean [SEM], 0.21; $P = .01$), executive function ($B = -0.90$; SEM, 0.31; $P = .01$), and global cognition ($B = -0.82$; SEM, 0.32; $P = .01$).

Conclusion: Among patients with cognitive symptoms, larger choroid plexus volume was associated with severity of cognitive impairment in the Alzheimer disease spectrum.

Online supplemental material is available for this article.

Alzheimer disease (AD), the most common form of dementia, is characterized by the accumulation of extracellular amyloid plaques and intracellular tau proteins. Both amyloid and tau depositions lead to neurodegeneration, ultimately causing cognitive decline and memory loss (1). Accumulating evidence suggests that the failure to clear these protein accumulations, rather than the overproduction of proteins, is responsible for AD development (2,3). Most suggested clearance pathways are linked to the cerebrospinal fluid (CSF), including degradation and cellular uptake, transport across the blood-brain barrier and blood-CSF barrier, interstitial fluid bulk flow, and CSF absorption into the circulatory and lymphatic systems (3).

The choroid plexus (CP) is a multifunctional structure that not only produces CSF but also forms the blood-CSF barrier by means of tight junctions between choroidal epithelial cells (4). The CP provides nutrients, a clearance system, and immune surveillance (4,5). It consists of a core of highly vascularized stroma with fenestrated capillaries and epithelial cells joined via tight junctions on the surface (5).

Distinctive CP structural changes have been reported in autopsy series of aged individuals and patients with AD. Such changes include flattening and atrophy of the epithelium, basal membrane thickening, vessel wall thickening, stromal fibrosis, and calcifications (6). Furthermore, in patients with AD, neurofibrillary tangle-like inclusions and β-amyloid deposits have been identified in the epithelial cells of the CP (7,8), with a significantly reduced CSF production rate (9). In addition, the CP has been suggested as a treatment target for AD (10).

In the CP, the fenestrated endothelial cells of the choroidal capillaries constitute the first layer of the blood-CSF barrier (11,12). Changes in permeability may lead to an increased flow of blood-borne toxic substances into the CSF

Abbreviations

AD = Alzheimer disease, *APOE4* = apolipoprotein E ε4 allele, CP = choroid plexus, CSF = cerebrospinal fluid, DCE = dynamic contrast-enhanced, MCI = mild cognitive impairment, MMSE = Mini-Mental State Examination, QSM = quantitative susceptibility mapping, SCI = subjective cognitive impairment, SEM = standard error of the mean, 3D = three-dimensional, V_p = fractional plasma volume, WMH = white matter hyperintensity

Summary

In patients along the Alzheimer disease clinical spectrum, choroid plexus volume and permeability were associated with severity of cognitive impairment at 3.0-T MRI of the brain.

Key Results

- In a retrospective study of 532 patients with cognitive impairment who underwent 3.0-T MRI of the brain, choroid plexus (CP) volume was greater in those with Alzheimer disease than in those without ($P < .001$).
- CP volume was negatively associated with the volume transfer constant ($r = -0.19$; $P = .03$) and fractional plasma volume ($r = -0.20$; $P = .02$).
- Higher CP volume was negatively associated with memory ($B = -0.67$; $P = .01$), executive function ($B = -0.90$; $P = .01$), and Mini-Mental State Examination *z*-score ($B = -0.82$; $P = .01$).

or a decreased flow of the essential nutrients from the blood into the CSF. CP susceptibility may also be affected by the calcifications reported in older individuals and in patients with AD (13).

Only a few MRI studies of the CP in older patients (>65 years) and patients with AD have been reported. One study reported that CP enlargement correlated with lower levels of CSF proteins in AD (14). Studies detailing in vivo imaging of structural and functional changes of the CP in AD remain lacking.

We therefore aimed to evaluate differences in CP volume, CP permeability, and CP susceptibility at various stages of cognitive impairment in the clinical AD spectrum.

Materials and Methods

Study Design and Patient Selection

This retrospective analysis of MRI data in patients with cognitive impairment was approved by our institutional review board (no. 2020–09–018), which waived the requirement for written informed consent (Appendix E1 [online]).

We considered patients from *(a)* an ongoing prospective multicenter cohort of consecutive patients with cognitive impairment who underwent DCE MRI between August 2017 and May 2020 at Konkuk University Medical Center, Seoul, Korea ($n = 158$), and *(b)* a dementia registry of consecutive patients diagnosed with cognitive impairment spectrum between January 2013 and May 2019 at Konkuk University Medical Center and with apolipoprotein E ε4 allele (*APOE4*) status information available ($n = 494$). Among the 158 patients in the prospective DCE MRI cohort, 52 with cognitive impairment and without dementia had been previously studied for permeability differences in the hippocampus and cerebral cortex (15,16). We excluded patients with dementia due to any cause other than AD, patients younger than 45 years of age, and those older than 90 years. Data sets without T1 volumetric images or with severe MRI artifacts were also excluded. A total of 94 patients had amyloid PET images available (Fig 1).

Probable AD and mild cognitive impairment (MCI) were diagnosed using criteria from the *Diagnostic and Statistical Manual of Mental Disorders*, fourth edition; the National Institute of Neurologic and Communicative Disorders and Stroke; the Alzheimer Disease and Related Disorders Association (17); and the articles by McKhann et al (18) and Petersen et al (19). Subjective cognitive impairment (SCI) was defined as impairment that did not meet the aforementioned criteria but included a subjective cognitive symptom reported by the patient (20). Early and late MCI were defined as a Clinical Dementia Rating Sum of Boxes of less than 1.5 and of 1.5 or greater, respectively (21).

Clinical Assessments

The patients' demographic characteristics, education level, comorbidities, global cognitive assessment scores (Mini-Mental State Examination [MMSE] score and Clinical Dementia Rating Sum of Boxes), *APOE4* genotyping result, and brain imaging findings were evaluated. A comprehensive neuropsychologic assessment was performed to evaluate the specific dysfunction in five cognitive domains: attention, visuospatial function, language, execution, and memory (22). The cognitive domain score was reported as a composite of the standardized scores of each cognitive domain subtest. Results obtained within 2 months of MRI were used for statistical analysis. Vascular risk factors were based on previous studies (15,23) (Appendix E1 [online]).

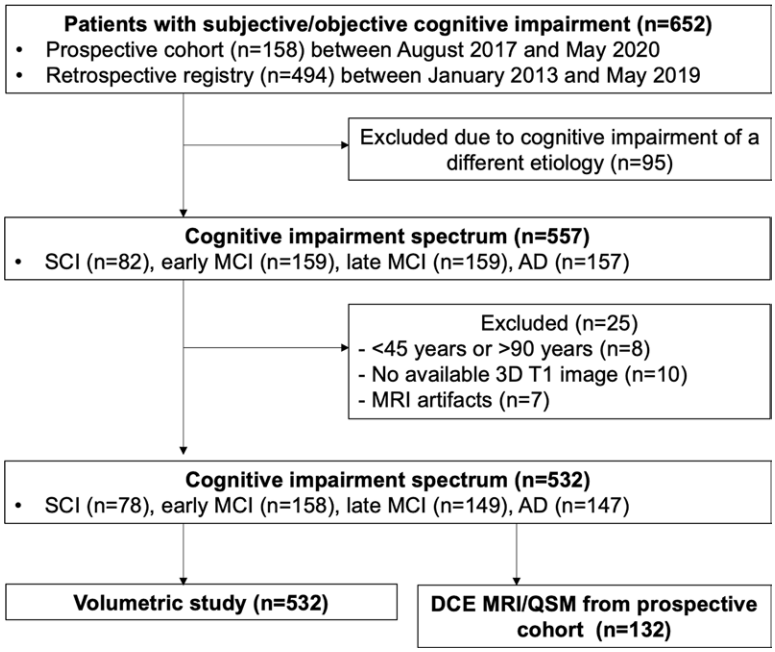

Figure 1: Flowchart of patient selection. AD = Alzheimer disease, DCE = dynamic contrast-enhanced, MCI = mild cognitive impairment, QSM = quantitative susceptibility mapping, SCI = subjective cognitive impairment, 3D = three-dimensional.

MRI Acquisition

MRI examinations were performed at 3.0 T using the same scanner with a 20-channel head coil (Magnetom Skyra; Siemens Healthineers) and a protocol including a three-dimensional (3D) 1-mm isovoxel T1-weighted sequence (repetition time/echo time/inversion time [msec], 2300/2.98/900), two-dimensional or 3D fluid-attenuated inversion-recovery images (9000/95/2500 or 5000/393/1800), 3D susceptibility-weighted images (29/20), or 3D multidynamic gradient-echo images (51/8.9; six echoes, with echo spacing of 4.09 msec).

A coronal DCE sequence (voxel size, 1.25 × 1.25 × 3 mm) was obtained with 60 dynamics, a time resolution of 10 seconds, and a standard dose of gadobutrol (Gadovist; Bayer Healthcare) (15). A precontrast T1-weighted gradient-echo MRI sequence (3.10/0.97) was obtained for T1 mapping (24) (Appendix E2 [online]).

MRI Analysis

MRI volumetric analysis.—Volumetric analysis was performed automatically using the Ministry of Food and Drug Safety of Korea–approved software Inbrain (Midas Information Technology), which is automatic volumetry software based on the FreeSurfer 6.0 platform (*https://surfer.nmr.mgh.harvard.edu*) and enhanced with a deep learning algorithm, as previously decribed (25–27). In a subset of 30 patients, we additionally obtained manual segmentations of CP volume to assess intermethod reliability. Two neuroradiologists (W.J.M. and Y.Y., with 21 years and 5 years of experience, respectively) independently manually segmented the CP in the lateral ventricle on the 3D T1-weighted volumetric images with use of ITK-SNAP software, version 3.8.0 (*http://www.itksnap.org*). The final corrected manual segmentation volume was determined by consensus of the two raters (Appendix E3 [online]).

The intracranial volume, cortical gray matter volume, lateral ventricle volume, CP volume, hippocampus volume, white matter hyperintensity (WMH) volume, deep WMH volume, and periventricular WMH volume were determined. All final automatic segmentation results were checked and approved without any manual correction by one neuroimaging researcher (S.L., with 9 years of experience). The regional volume was expressed as the ratio of the regional volume to the total intracranial volume (Fig 2).

DCE imaging analysis.—Two permeability parameters (volume transfer constant [ie, K^{trans}] and fractional plasma volume [ie, V_p]) were calculated from DCE MRI data by using the Patlak model, as previously described (15,24,28). The CP DCE parameters were obtained by means of CP mask coregistration from T1-weighted volumetric images to the

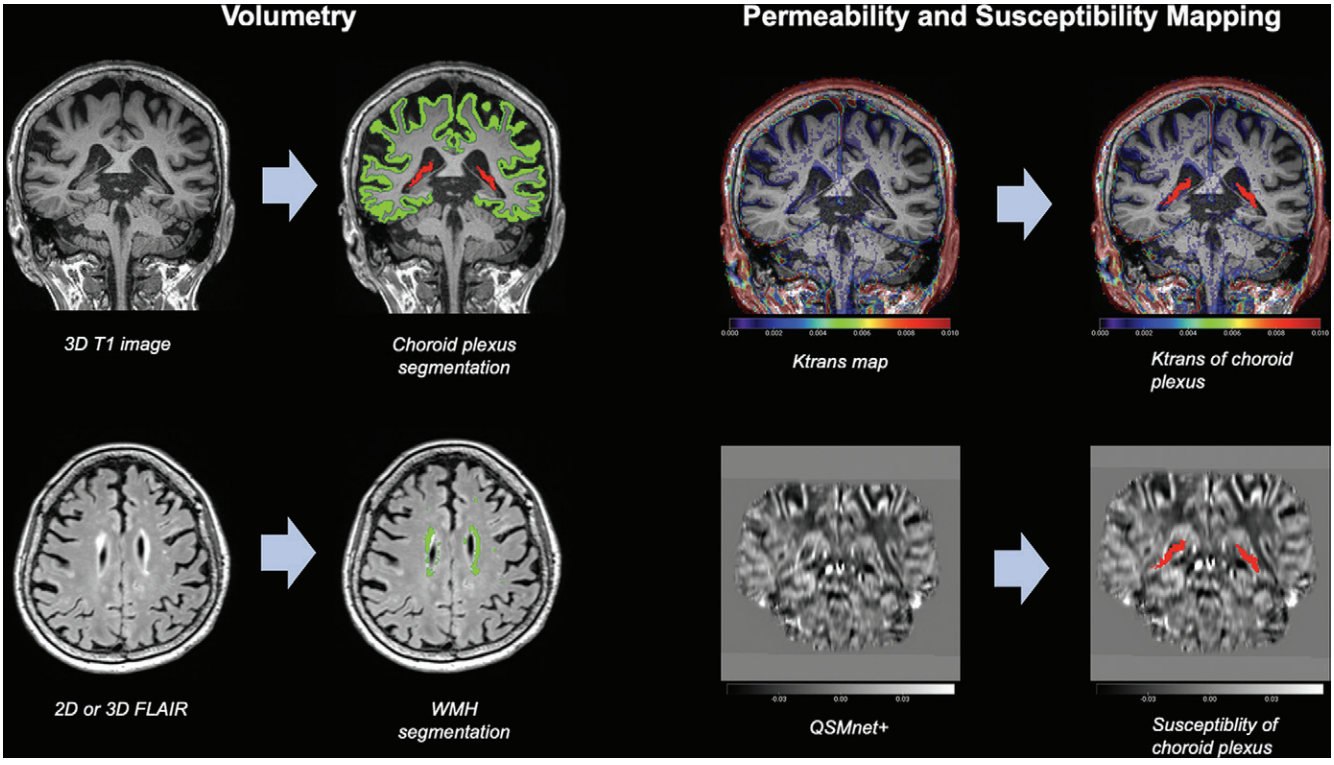

Figure 2: MRI processing steps. For volumetry (left), choroid plexus (CP) volume (red) and cerebral cortex volume (green) are segmented from T1-weighted volumetric images by using an automatic volumetric software (Inbrain) based on the FreeSurfer 6.0 platform (upper row). White matter hyperintensity (WMH) volumes (green) are also segmented from three-dimensional (3D) or two-dimensional (2D) fluid-attenuated inversion-recovery (FLAIR) images by using the same software (lower row). The segmented mask volumes are binary. For permeability and susceptibility mapping (right), permeability values (volume transfer constant [K^{trans}] and fractional plasma volume) are obtained from dynamic contrast-enhanced MRI scans by using the Patlak model, and CP permeability values are extracted with use of coregistration of the segmented CP (red) of T1-weighted images to the parametric map using a mutual information-based algorithm (upper row). The color scale bar represents the volume transfer constant (in min^{-1}). CP susceptibility measures are generated in an analogous manner. Quantitative susceptibility mapping (QSM) is obtained from multidynamic multiecho images by using QSMnet$^+$ (lower row). The grayscale bar represents susceptibility in parts per million.

DCE parameter map by using a mutual information-based algorithm (Appendix E3 [online]).

Analysis of quantitative susceptibility mapping images.—Quantitative susceptibility mapping (QSM) images were generated as previously described (29–31). The reconstructed QSM image was zero-referenced to the mean CSF susceptibility by dividing voxel values by the mean value of the lateral ventricle region (32). CP susceptibility was extracted by overlaying the CP mask on the QSM image. CP segmentation was coregistered from T1-weighted MRI space to QSM space before the overlay, and the mean susceptibility was extracted from the CP region (Appendix E3 [online]).

Imaging analysis for microvascular factors.—Microvascular MRI factors (WMH visual scales, lacunes, and microbleeds) were assessed as previously described (15,23). The number of microbleeds (<10 mm in diameter, with associated blooming at susceptibility-weighted imaging and on QSM images) was used as an imaging covariate in the subsequent logistic regression analysis for determining independent predictors of worse global cognition (Appendix E3 [online]).

Statistical Analysis

All statistical analyses were performed using SPSS software, version 25.0 (IBM). $P < .05$ was considered indicative of statistically significant difference, and P values were Bonferroni-corrected for multiple comparisons. Intermethod reliability of CP segmentation was assessed with use of the intraclass correlation coefficient (two-way mixed model, single measure, absolute agreement). Kolmogorov-Smirnov tests, analysis of variance or the Kruskal-Wallis test, and the Jonckheere trend test were used for continuous variables; the χ^2 test was used for categorical variables. A two-way analysis of covariance adjusted for age, sex, education, and/or high vascular risk burden (at least two vascular risk factors) was used to evaluate the main effect of diagnosis and *APOE4* status or a vascular risk factor or amyloid positivity on the CP volume. After adjustment for the confounding effects of age, sex, and sequence difference (two-dimensional or 3D fluid-attenuated inversion recovery for WMH), parametric and nonparametric partial correlation and multivariable linear regression analyses were performed for the relationship between CP volume and other imaging measures. The relationship between CP volume and cognitive decline (domain-specific or global) was evaluated using univariable and multivariable linear regression analyses with a forward stepwise approach. Finally, independent predictors for worse global cognition (MMSE z-score cutoff value of −1.5) were determined using multivariable logistic regression analyses to evaluate demographic and imaging variables. (Appendix E4 [online]).

Results

Clinical and Demographic Characteristics

Among the 652 patients considered, 120 were excluded: patients with dementia due to any cause other than AD ($n = 95$), patients younger than age 45 years or older than 90 years ($n = 8$), patients without T1-weighted volumetric images ($n = 10$), and patients whose examinations had severe MRI artifacts ($n = 7$). After exclusions, we evaluated 532 patients with cognitive impairment (mean age, 72 years ± 9 [SD]; 388 women): 78 with SCI, 158 with early MCI, 149 with late MCI, and 147 with AD (Fig 1). Among them, the DCE MRI prospective cohort comprised 132 patients (mean age, 72 years ± 7; 85 women). Patients with AD were older and had lower education levels than the rest of the patients ($P < .001$ for both). The *APOE4* variant was more prevalent with increasing cognitive impairment ($P < .001$). We found no differences in sex ($P = .87$), vascular risk burdens ($P = .32$), or depression ($P = .14$) between the groups. Patients with late MCI or AD had lower MMSE scores than those in the SCI or early MCI groups (all $P < .001$) (Table 1).

Effects of Diagnosis, Age, Sex, and Vascular Risk Factors on CP Volume

Inbrain-based segmentation of CP volume demonstrated an excellent intraclass correlation coefficient (0.92; 95% CI: 0.84, 0.96; $P < .001$) with the manual segmentation of CP volume as the reference standard.

Cortical gray matter, lateral ventricle, CP, hippocampus, and WMH volumes differed among groups (all $P < .001$) (Tables 2, E1 [online]). Patients with AD had higher CP volume (ratio of intracranial volume × 10^3, 1.3 ± 0.4) than patients with late MCI (1.1 ± 0.3), early MCI (1.0 ± 0.3), and SCI (0.9 ± 0.3) (all $P < .001$) and lower hippocampus volume (4.2 ± 0.6) than patients with late MCI (4.7 ± 0.6), early MCI (5.0 ± 0.6), and SCI (5.2 ± 0.5) (all $P < .001$) (Fig 3). We found a difference in hippocampus volume ($P = .03$) but no evidence of difference in CP volume ($P = .43$, post hoc Tukey test) between the SCI and early MCI groups (Fig 4).

In an evaluation of the main effect of diagnosis and *APOE4* status after adjustment for age, sex, education, and vascular risk, the CP volume differed between diagnostic groups ($F = 18.7$; $P < .001$), but we found no evidence for a difference based on *APOE4* status ($P = .49$). Furthermore, older age (>75 years) ($F = 89.0$; $P < .001$) and male sex ($F = 38.2$; $P < .001$) were associated with higher CP volume (Fig E1 [online]).

When we evaluated the effect of each vascular risk factor after adjusting for covariates, hypertension ($F = 7.72$; $P = .01$), diabetes ($F = 4.79$; $P = .03$), and cardiovascular disease history ($F = 4.62$; $P = .03$) were associated with higher CP volume (Fig E2 [online]).

After correction for covariates, CP volume was associated with diagnosis ($F = 3.43$; $P = .02$); however, we found no evidence of an association with amyloid positivity ($F = 0.01$; $P = .98$) (Fig E3 [online]).

Relationship between CP Volume and MRI Parameters

A strong correlation was identified between CP volume and the lateral ventricle volume ($r = 0.63$; $P < .001$), cortex volume ($r = −0.37$; $P < .001$), hippocampus volume ($r = −0.28$; $P < .001$), WMH volume ($r = 0.22$; $P < .001$), and periventricular WMH volume ($r = 0.31$; $P < .001$). The correlation between CP and periventricular WMH volumes was stronger in patients with AD ($r = 0.46$; $P < .001$) than in patients with early MCI ($r = 0.17$; $P = .03$) or late MCI ($r = 0.24$; $P = .004$) (Table E2 [online]).

Table 1: Clinical and Demographic Characteristics of Patients according to Disease Stage

Characteristic	SCI (*n* = 78)	Early MCI (*n* = 158)	Late MCI (*n* = 149)	AD (*n* = 147)	*P* Value
Age (y) *	69 ± 8	70 ± 9	73 ± 8	76 ± 8	<.001
Sex					.87
Female	57 (73)	119 (75)	107 (72)	105 (71)	
Male	21 (27)	39 (25)	42 (28)	42 (29)	
APOE4 status	14 (18)	33 (21)	50 (34)	62 (42)	<.001
Amyloid PET positivity†	8/13 (62)	21/31 (68)	18/27 (67)	18/23 (691)	.72
Education (y)‡	10 (6–14)	9 (6–14)	9 (6–12)	6 (3–12)	<.001
Hypertension	32 (41)	66 (42)	71 (48)	78 (53)	.17
Type 2 diabetes mellitus	11 (14)	29 (18)	41 (28)	35 (24)	.07
Dyslipidemia	22 (28)	65 (41)	45 (30)	43 (29)	.07
Cardiovascular disease	11 (14)	19 (12)	22 (15)	8 (5)	.06
CDR-SB‡	0.5 (0.5–1.0)	0.5 (0.5–1.0)	2 (1.5–2.5)	4.5 (3.0–5.5)	<.001
MMSE score‡	28 (27–30)	27 (26–29)	25 (21–27)	20 (16–22)	<.001
MMSE *z*-score*	0.22 ± 0.91	−0.43 ± 1.09	−1.83 ± 1.82	−3.34 ± 2.44	<.001
Execution *z*-score*	0.46 ± 0.97	−0.61 ± 1.28	−1.61 ± 1.60	−2.47 ± 2.00	<.001
Attention *z*-score*	0.32 ± 0.82	−0.20 ± 0.89	−0.32 ± 0.86	−0.52 ± 1.01	<.001
Language *z*-score*	0.32 ± 0.92	−0.10 ± 1.14	−0.73 ± 1.72	−1.20 ± 2.14	<.001
Memory *z*-score*	0.34 ± 0.82	−0.64 ± 1.02	−1.59 ± 1.18	−2.39 ± 1.20	<.001
Visuospatial *z*-score*	0.16 ± 0.83	−0.37 ± 1.28	−0.89 ± 1.51	−1.88 ± 2.45	<.001

Note.—Unless otherwise noted, data are numbers of patients, with percentages in parentheses. AD = Alzheimer disease, *APOE4* = apolipoprotein E ε4 allele, CDR-SB = Clinical Dementia Rating Sum of Boxes, MCI = mild cognitive impairment, MMSE = Mini-Mental State Examination, SCI = subjective cognitive impairment.

* Data are means ± SDs.

† Amyloid PET data were available for 94 of 532 study patients (17.7%).

‡ Data are medians, with IQRs in parentheses.

Table 2: Volumetric and Dynamic Contrast-enhanced MRI Measures according to Disease Stage Group in All Patients

Total (*n* = 532)	SCI (*n* = 78)	Early MCI (*n* = 158)	Late MCI (*n* = 149)	AD (*n* = 147)	*P* Value
ICV (mL)	1468 ± 133	1459 ± 143	1436 ± 147	1439 ± 148	.27
Cortex volume (mL)	422 ± 34	419 ± 34	403 ± 39	384 ± 37	<.001
LV volume (mL)	27 ± 12	30 ± 16	34 ± 16	47 ± 22	<.001*
CP volume (mL)	1.4 ± 0.5	1.5 ± 0.5	1.6 ± 0.5	1.9 ± 0.6	<.001
HV (mL)	7.6 ± 0.8	7.2 ± 0.8	6.6 ± 0.9	6.0 ± 0.6	<.001
Total WMH volume (mL)*	7.2 (5.5–10.4)	8.1 (5.4–14.1)	9.8 (6.5–16.1)	13.4 (8.2–22.0)	<.001
Periventricular WMH volume (mL)*	5.9 (4.0–11.6)	6.0 (4.0–11.6)	7.2 (4.8–12.1)	10.0 (5.9–18.2)	<.001
Cortex (ratio of ICV)	0.29 ± 0.02	0.29 ± 0.02	0.28 ± 0.02	0.27 ± 0.02	<.001
LV (ratio of ICV × 10^3)*	16.6 (12.1–23.0)	18.4 (13.3–24.7)	21.6 (16.4–30.1)	29.9 (20.6–41.4)	<.001
CP (ratio of ICV × 10^3)	0.9 ± 0.3	1.0 ± 0.3	1.1 ± 0.3	1.3 ± 0.4	<.001
HV (ratio of ICV × 10^3)	5.2 ± 0.5	5.0 ± 0.6	4.7 ± 0.6	4.2 ± 0.6	<.001
WMH (ratio of ICV × 10^3)*	5.1 (3.9–7.8)	5.5 (3.9–9.3)	6.9 (4.6–11.1)	9.2 (5.8–15.1)	<.001
Periventricular WMH (ratio of ICV × 10^3)*	3.9 (3.0–5.5)	4.0 (2.9–7.6)	5.1 (3.4–8.4)	6.8 (4.4–12.7)	<.001

Note.—Unless otherwise indicated, data are means ± SDs. AD = Alzheimer disease, CP = choroid plexus, HV = hippocampus volume, ICV = intracranial volume, LV = lateral ventricle, MCI = mild cognitive impairment, SCI = subjective cognitive impairment, WMH = white matter hyperintensity.

* Data are medians, with IQRs in parentheses.

After adjustment for *APOE4* status, education, cortex volume, hippocampus volume, and periventricular WMH volumes, lateral ventricle volume (B = 0.02; standard error of the mean [SEM], 0.01), age (B = 0.01; SEM, 0.01; $P < .001$), sex (B = −0.88; SEM, 0.02; P = .01), presence of severe impairment (late MCI and AD) (B = 0.07; SEM, 0.02; P = .01), and

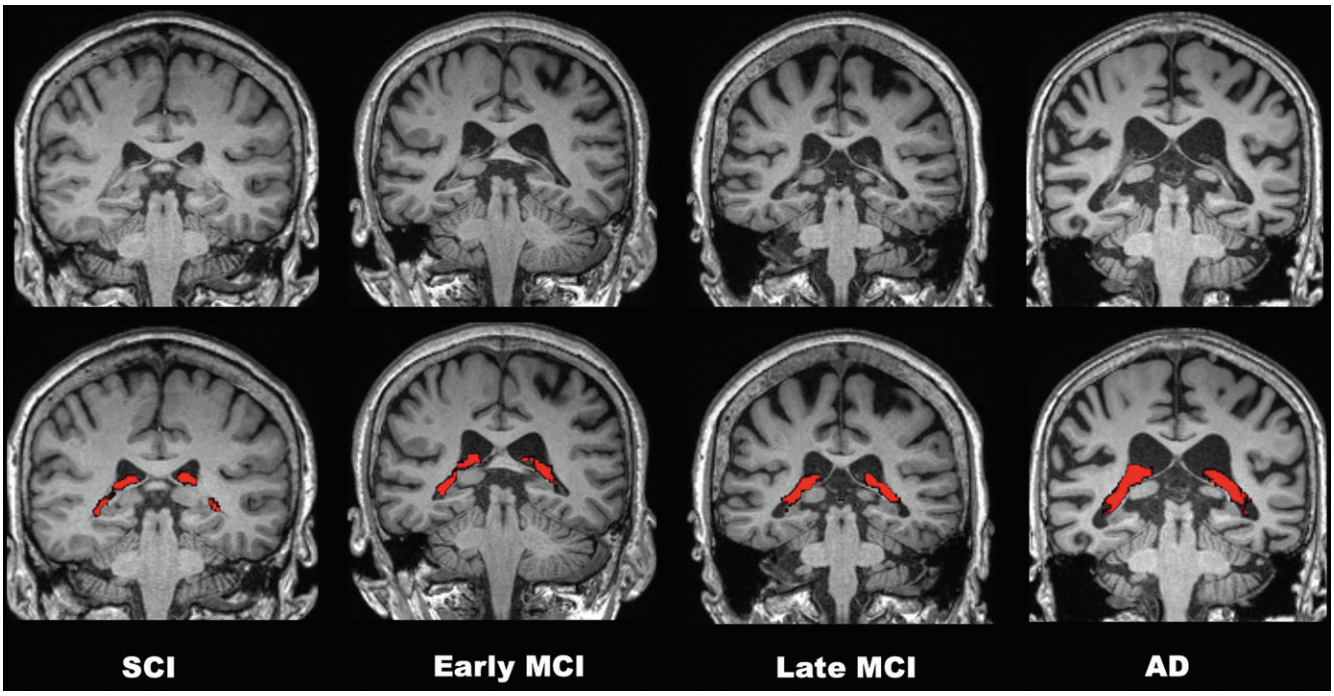

Figure 3: Comparisons of four representative 3.0-T brain MRI scans of choroid plexus (CP) volume (red) according to disease stage over the cognitive impairment spectrum. CP volume is greater in the patient with Alzheimer disease (AD) than in those with subjective cognitive impairment (SCI) or mild cognitive impairment (MCI). All patients were 75-year-old women.

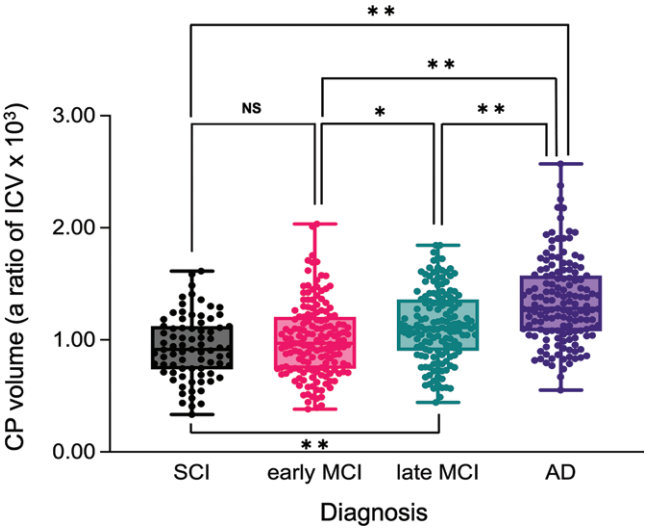

Figure 4: Box plots of choroid plexus (CP) volumes in patients with different stages of cognitive impairment (n = 532). The CP volume (expressed as the ratio of CP volume to intracranial volume [ICV]) in patients with late mild cognitive impairment (MCI) is higher by 21.4% and 13.0% compared with volume in patients with subjective cognitive impairment (SCI) and early MCI, respectively ($P < .001$ and $P = .01$); the volume in patients with Alzheimer disease (AD) is higher by 43.6% and 33.7% compared with that in patients with SCI and early MCI, respectively ($P < .001$). However, CP volumes did not significantly differ between the SCI and early MCI groups ($P = .51$). The horizontal line in each box plot indicates the median, and the box corresponds to the IQR. The whiskers indicate minimum and maximum values in the data. * = $P < .05$ and ** = $P < .001$. P values were corrected for multiple comparisons. NS = not significant.

hypertension (B = 0.05; SEM, 0.02; P = .03) were predictive factors for CP volume (R^2 = 0.565; F (5, 526) = 135.4; $P < .001$).

CP Permeability and Susceptibility

In the DCE MRI prospective cohort (n = 132), CP volume was greater in patients diagnosed with AD than in those not diagnosed with AD ($P < .001$) (Table 3; Table E3 [online]). CP K^{trans} differed among groups, with lower values in patients with AD than in those with late MCI (P = .04). Lower CP V_p was associated with worse cognitive impairment (P = .02, Jonckheere trend test) (Fig 5). After correction for age and sex, K^{trans} was lower in patients with larger CP volumes in the early MCI group (r = −0.39; P = .01) and the whole group (r = −0.19; P = .03). Lower V_p was associated with larger CP volume in the AD group (r = −0.51; P = .01) and the whole group (r = −0.20; P = .02).

In contrast, we found no evidence that CP susceptibility differed between groups (P = .73) and no association between CP susceptibility and CP volume after correction for age and sex (r = −0.15; P = .10) (Fig 6; Table E4 [online]).

Relationship between CP Volume and Cognition

Cognitive domain scores were available for 411 patients. Among these patients, CP volume was negatively correlated with memory (B = −0.99; SEM, 0.20; $P < .001$), executive function (B = −1.24; SEM, 0.26; $P < .001$), and visuospatial function (B = −0.94; SEM, 0.26; $P < .001$).

After adjustment for demographic imaging covariates, CP volume was negatively associated with memory (B = −0.67; SEM, 0.21; P = .01), executive function (B = −0.90; SEM, 0.31; P = .01), and MMSE z-score (B = −0.82; SEM, 0.32; P = .01).

Table 3: Volumetric and DCE MRI Measures according to Disease Stage Group in the DCE MRI Cohort

Subgroup (n = 132)	SCI (n = 23)	Early MCI (n = 46)	Late MCI (n = 35)	AD (n = 28)	P Value
ICV (mL)	1533.2 ± 159.8	1449.2 ± 147.0	1484.5 ± 179.7	1426.0 ± 155.4	.07
Cortex volume (mL)	428.5 ± 43.6	415.2 ± 34.0	410.2 ± 42.1	382.1 ± 26.7	<.001
LV volume (mL)	32.8 ± 16.8	32.0 ± 11.7	35.5 ± 16.7	47.9 ± 20.2	<.001
CP volume (mL)	1.7 ± 0.6	1.6 ± 0.5	1.7 ± 0.4	2.0 ± 0.5	.001
HV (mL)	7.7 ± 1.2	7.2 ± 0.8	6.6 ± 1.1	6.0 ± 1.0	<.001
Total WMH volume (mL)*	6.9 (5.3–11.3)	5.6 (4.5–11.6)	8.6 (4.5–12.6)	12.9 (6.3–18.4)	.04
Periventricular WMH volume (mL)*	6.1 (4.6–9.5)	5.0 (3.9–10.4)	7.0 (4.1–12.0)	12.1 (5.8–17.8)	.02
Cortex (ratio of ICV)	0.28 ± 0.2	0.29 ± 0.2	0.28 ± 0.2	0.27 ± 0.2	<.001
LV (ratio of ICV × 10^3)*	19.2 (14.5–28.8)	20.8 (17.1–25.5)	22.0 (16.2–29.1)	30.2 (23.3–40.5)	<.001
CP (ratio of ICV × 10^3)	1.1 ± 0.3	1.1 ± 0.3	1.2 ± 0.3	1.4 ± 0.3	<.001
HV (ratio of ICV × 10^3)	5.0 ± 0.7	5.0 ± 0.7	4.5 ± 0.6	4.2 ± 0.5	<.001
WMH (ratio of ICV × 10^3)*	4.5 (3.5–7.0)	3.9 (3.0–7.5)	5.6 (3.0–8.9)	8.4 (4.9–13.9)	.02
Periventricular WMH (ratio of ICV × 10^3)*	4.0 (3.0–6.1)	3.7 (2.7–6.7)	4.6 (2.7–7.6)	8.0 (4.4–12.7)	.01
K^{trans} of CP ($\times 10^{-3} \cdot min^{-1}$)*	0.56 (0.31–1.65)	0.66 (0.18–1.26)	1.16 (0.41–2.33)	0.37 (0.18–1.12)	.04
V_p of CP (%)*	10.1 (7.5–12.1)	10.2 (8.0–12.8)	9.0 (7.0–12.2)	8.4 (4.7–10.5)	.17
Susceptibility of CP (ppb)	−2.6 ± 5.4	−2.0 ± 5.6	−1.6 ± 5.4	−2.1 ± 5.4	.73

Note.—Unless otherwise indicated, data are means ± SDs. AD = Alzheimer disease, CP = choroid plexus, DCE = dynamic contrast-enhanced, HV = hippocampus volume, ICV = intracranial volume, K^{trans} = volume transfer constant, LV = lateral ventricle, MCI = mild cognitive impairment, ppb = parts per billion, SCI = subjective cognitive impairment, V_p = fractional plasma volume, WMH = white matter hyperintensity.

* Data are medians, with IQRs in parentheses.

CP Volume as an Independent Diagnostic Marker of Cognitive Status

When CP measure was added to the current imaging measures for AD (hippocampus atrophy, WMH load, and microbleed load) in the model, logistic regression indicated that hippocampus volume ($P < .001$) and CP volume ($P < .001$), along with female sex ($P = .04$) and the *APOE4* variant ($P < .001$), were significant predictors of worse global cognition (MMSE z-score of −1.5 or less), whereas WMH load ($P = .39$) and number of microbleeds ($P = .23$) were not. The area under the receiver operating characteristic curve of the model was 0.77 (95% CI: 0.73, 0.81) (Table 4).

When CP permeability was added in the model, hippocampus volume ($P < .001$) and CP volume ($P = .04$) were independent predictors of worse cognition, whereas WMH load ($P = .38$), microbleed number ($P = .33$), and CP permeability ($P = .31$) were not. The area under the receiver operating characteristic curve of the model was 0.83 (95% CI: 0.75, 0.89) (Table 4).

Discussion

Growing evidence suggests that the choroid plexus (CP) may play an important role in Alzheimer disease, but its role in cognitive impairment remains unclear. In this study, CP volume was associated with the stage of cognitive impairment (severity) ($P < .001$). Age ($P < .001$), male sex ($P < .001$), and hypertension ($P = .01$) were associated with a larger CP volume, whereas amyloid positivity was not ($P = .98$). CP permeability (volume transfer constant and fractional plasma volume) was negatively correlated with CP volume ($r = -0.19$ [$P = .03$] and $r = -0.20$ [$P = .02$]), but CP susceptibility was not ($r = -0.15$; $P = .10$). CP volume was identified as an independent predictor of Mini-Mental State Examination (MMSE) score ($P = .01$), memory ($P = .01$), and executive function ($P = .01$). We also found that CP volume was an additional independent factor predicting worse cognition (MMSE z-score of −1.5 or less), along with hippocampus volume ($P < .001$), female sex ($P = .04$), and apolipoprotein E ε4 allele carrier status ($P < .001$).

The volume differences of the CP in our study are consistent with those observed by Tadayon et al (14). In that study, the AD group had larger CP volumes than the healthy controls and the MCI group; however, CP volume did not differ between the other groups, which may be attributed to image acquisition with a 1.2-mm isotropic spatial resolution on different scanners at multiple institutions (14). In contrast, in our study, which used 1-mm isotropic resolution images on the same scanner, differences in CP volume were observed between the various groups of patients with cognitive impairment, which may be due to a higher sensitivity for detecting differences in CP volume. The higher CP volume in patients with AD-related cognitive impairment may be due to a higher degree of stromal fibrosis, stromal dystrophic calcification, blood vessel thickening, or inflammation, which may eventually lead to failure of CSF production and clearance (6,8,9). Those changes were also reported in aged patients (6,7), consistent with the age dependency of CP volume identified in our study.

The CP contains estrogen, progesterone, and androgen receptors (33). In a recent study on healthy controls and patients

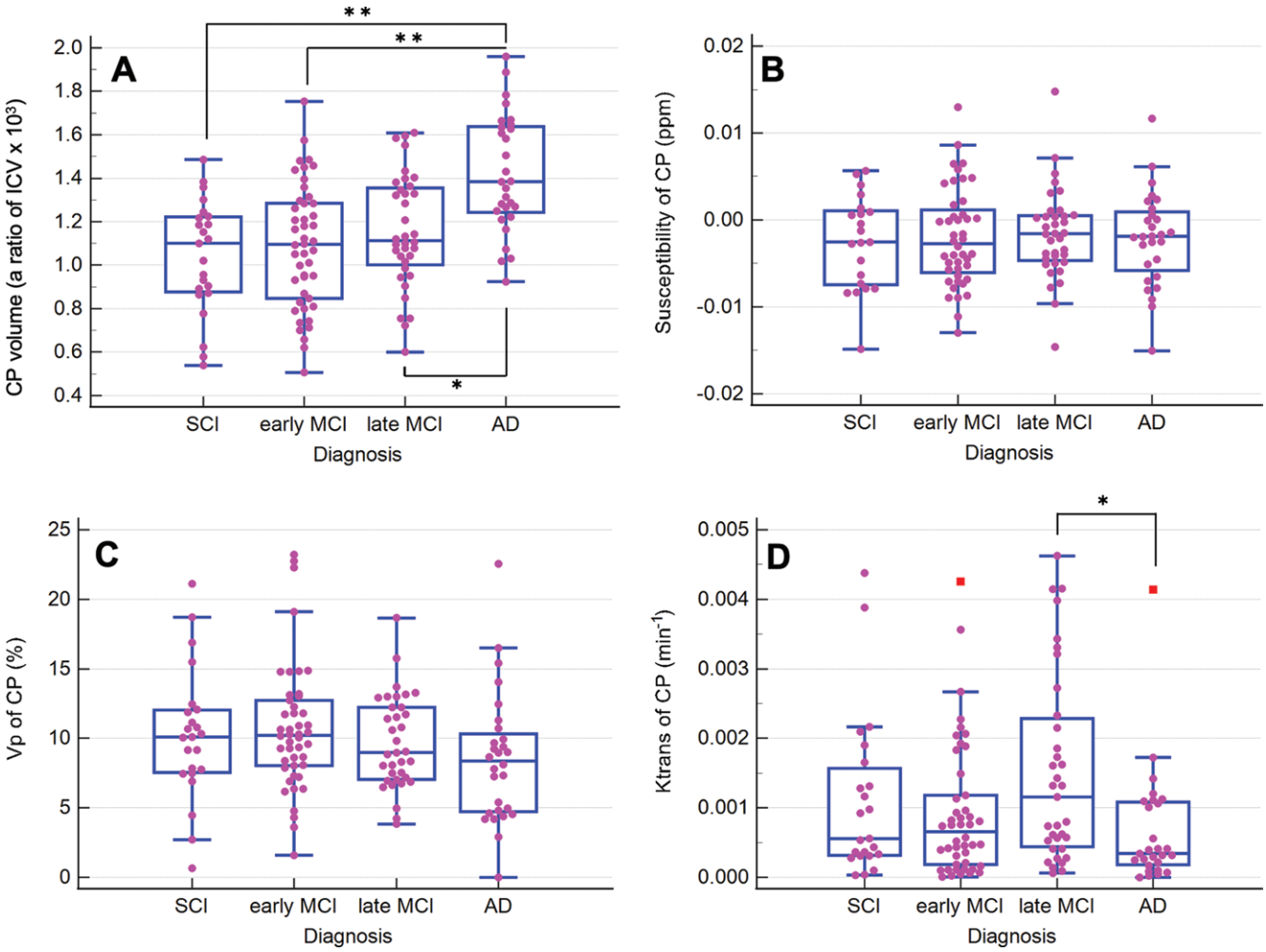

Figure 5: Box plots show **(A)** structural volume, **(B)** susceptibility, and **(C, D)** permeability characteristics of the choroid plexus (CP) in the dynamic contrast-enhanced MRI cohort along the cognitive impairment spectrum (n = 132). Higher CP volume was observed in patients with Alzheimer disease (AD) than in those without dementia, with lower CP permeability (volume transfer constant [K^{trans}]) in patients with AD than in those with late mild cognitive impairment (MCI). Fractional plasma volume (V_p) of CP tended to be lower with worse cognitive impairment status (P = .02, Jonckheere trend test). In contrast, CP susceptibility did not differ between groups (P = .73). The horizontal line in each box plot indicates the median, and the box corresponds to the IQR. The whiskers indicate minimum and maximum values in the data. The data points represented by red squares are outliers above the 3rd quartile + 3 × IQR. * = $P < .05$ and ** = $P < .001$. P values were corrected for multiple comparisons. ICV = intracranial volume, ppm = parts per million, SCI = subjective cognitive impairment.

with multiple sclerosis, no sex difference was observed for CP volume (34). However, the sex-related differences in CP volume in our study agree with previous studies reporting sex differences in CSF flow dynamics (35), density (36), and composition (33).

In a previous study in rats, arterial hypertension induced CP alteration and augmented disruption of the blood-brain barrier and blood-CSF barrier (37). Therefore, hypertension may be an underlying cause of CP abnormality. However, in our study, CP changes were not associated with the *APOE4* variant, a risk factor for AD and for vascular disease (1,15). CP is a site of production of the cholesterol transporter apolipoprotein E in the brain. *APOE4* reduces the efficient transport of CP/CSF-derived apolipoprotein E to the brain via perivascular spaces by the glymphatic fluid transporting system (38). The relationship between CP, *APOE4*, and the glymphatic system has not yet been elucidated.

Our results suggest that CP abnormality is not just a secondary finding of lateral ventricular enlargement but an independent process. Although CP volume strongly correlated with lateral ventricular volume, it was also associated with age, sex, and permeability changes. In addition, no relationship between CP volume and amyloid PET findings was identified, whereas CP volume and cognitive severity were closely correlated, suggesting that CP abnormality may be more closely related to tau abnormality and/or neurodegeneration than to amyloid abnormality (1). However, the cause-and-effect relationship of the CP in pathologic features of AD remains unclear.

In our study, CP permeability was reduced in patients with AD compared with those not diagnosed with AD. A weak negative correlation between CP permeability and volume was also identified in the total study sample. A small case series (n = 15) reported that capillary permeability of CP was associated with age (39). Conversely, our results suggest a more complex relationship between CP permeability and CP volume. Although CP permeability correlated with CP volume in patients with early MCI in our study, this correlation was not observed in

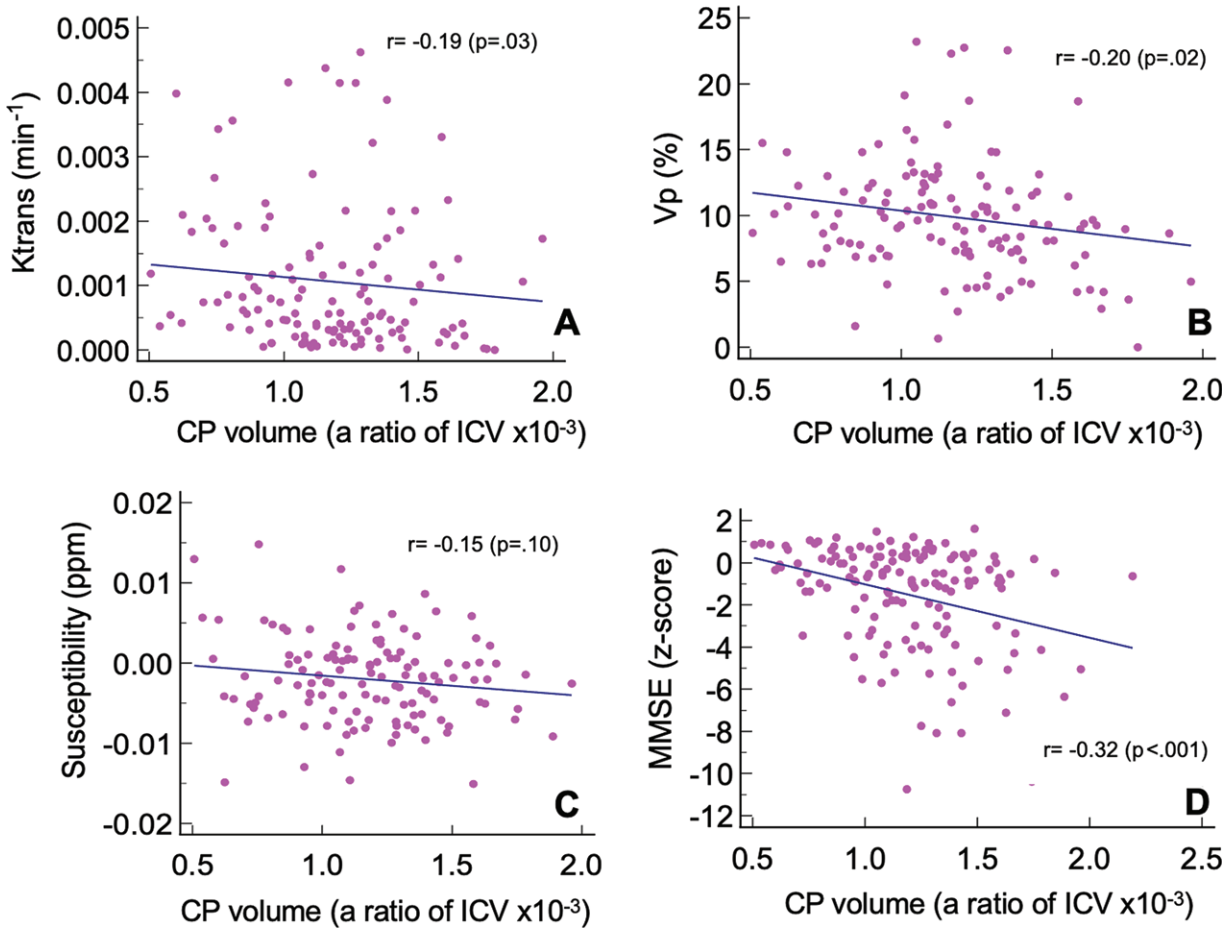

Figure 6: Relationship between the choroid plexus (CP) volume and imaging or cognitive parameters in the dynamic contrast-enhanced MRI cohort along the cognitive impairment spectrum (n = 132). **(A–D)** Scatterplots show significant association of large CP volume with lower volume transfer constant (K^{trans}), lower fractional plasma volume (V_p), and lower Mini-Mental State Examination (MMSE) z-score. The r values are partial correlation coefficients after correction for age and sex. ICV = intracranial volume, ppm = parts per million.

Table 4: Relationship between Demographic and Imaging Measures and Worse Global Cognition

	Model 1		Model 2		Model 3	
Predictor	Odds Ratio	*P* Value	Odds Ratio	*P* Value	Odds Ratio	*P* Value
Age (per y)	1.00 (0.97, 1.03)	.89	0.98 (0.95, 1.01)	.17	0.94 (0.85, 1.03)	.18
Female sex	1.36 (0.83, 2.24)	.22	1.76 (1.04, 2.98)	.04	0.64 (0.22, 1.82)	.40
APOE4 carrier	2.56 (1.62, 4.03)	<.001	2.64 (1.66, 4.21)	<.001	2.03 (0.75, 5.48)	.16
Education (>6 y)	0.73 (0.47, 1.14)	.17	0.79 (0.50, 1.24)	.30	0.83 (0.30, 2.24)	.71
Hippocampus volume (ratio of ICV × 10^3)	0.31 (0.21, 0.45)	<.001	0.36 (0.24, 0.53)	<.001	0.20 (0.08, 0.5)	<.001
WMH volume (ratio of ICV × 10^3)	1.02 (0.99, 1.05)	.14	1.01 (0.99, 1.04)	.39	1.03 (0.96, 1.10)	.38
Microbleed (no.)	1.03 (0.99, 1.07)	.12	1.02 (0.99, 1.07)	.23	1.09 (0.92, 1.30)	.33
CP volume (ratio of ICV × 10^3)			4.52 (2.10, 9.76)	<.001	7.17 (1.07, 48.11)	.04
CP K^{trans} ($\times 10^{-3} \cdot min^{-1}$)					0 (0, 0)	.31

Note.—Data are the exponentiation of the regression coefficients, which are odds ratios; data in parentheses are 95% CIs. Volumes of the hippocampus, white matter hyperintensity (WMH), and choroid plexus (CP) are presented as the ratio to intracranial volume (ICV) (multiplied by 10^3). Worse cognition is defined as Mini-Mental State Examination z-score of −1.5 or lower. *APOE4* = apolipoprotein E ε4 allele, K^{trans} = volume transfer constant.

patients with SCI, late MCI, or AD. CP permeability changes could have a nonlinear relationship with disease severity, similar to that seen with amyloid deposition in AD (1).

The relationship between V_p and cognitive impairment was more straightforward. Typically, local blood flow in the CP is the highest in the brain (40). Upregulated vascular endothelial growth factor

gene expression in patients with AD suggests impaired CP permeability and flow (41). Our results suggest that the capillary blood flow of the CP is lower with higher CP volume in patients with AD.

CP calcification has been reported in older patients (42); therefore, CP susceptibility was expectedly lower with increasing age and cognitive impairment. The lack of group difference in susceptibility in our study implies that CP enlargement may be independent of CP calcification.

We identified CP volume as an independent predictor of the MMSE *z*-score, which suggests that CP volume can be used as an imaging marker for clinical prognosis and staging. Furthermore, CP volume was associated with executive and memory function, indicating its potential use as an imaging marker for specific cognitive domain dysfunctions.

Our study had several limitations. First, because this was a cross-sectional study, temporal relationships could not be studied. Second, correlation analyses with amyloid and tau PET images were not performed in all patients (43). Third, despite the high intermethod reliability between our automatic CP volume segmentation and manual segmentation in a subgroup test, manual segmentation is still considered the reference standard for CP volume measurement.

In conclusion, choroid plexus (CP) volume was higher in more advanced cognitive impairment among patients with cognitive impairment who underwent 3.0-T MRI of the brain. Alterations in CP permeability were associated with disease severity. CP volume and permeability may be potential imaging markers for cognitive impairment in Alzheimer disease, independent of amyloid abnormality or neurodegeneration. Further validation and longitudinal studies are required to determine whether CP volume can be used in combination with other volumetric measures as a surrogate parameter for cognitive decline.

Acknowledgment: The authors thank Jinho Yang, MD, of the Department of Radiology of Konkuk University Medical Center for participating in the visual assessment of microbleeds at MRI.

Author contributions: Guarantors of integrity of entire study, **H.J.K., W.J.M.**; study concepts/study design or data acquisition or data analysis/interpretation, all authors; manuscript drafting or manuscript revision for important intellectual content, all authors; approval of final version of submitted manuscript, all authors; agrees to ensure any questions related to the work are appropriately resolved, all authors; literature research, **J.D.C., Y.Y., W.J.M.**; clinical studies, **J.D.C., Y.M., H.J.K., W.J.M.**; experimental studies, **H.J.K., Y.Y., W.J.M.**; statistical analysis, **J.D.C., S.L., W.J.M.**; and manuscript editing, **J.D.C., Y.Y., S.L., W.J.M.**

Data sharing: Data generated or analyzed during the study are available from the corresponding author by request.

Disclosures of conflicts of interest: J.D.C. No relevant relationships. **Y.M.** No relevant relationships. **H.J.K.** No relevant relationships. **Y.Y.** No relevant relationships. **S.L.** No relevant relationships. **W.J.M.** No relevant relationships.

References

1. van der Kant R, Goldstein LSB, Ossenkoppele R. Amyloid-β-independent regulators of tau pathology in Alzheimer disease. Nat Rev Neurosci 2020;21(1):21–35.
2. Mawuenyega KG, Sigurdson W, Ovod V, et al. Decreased clearance of CNS beta-amyloid in Alzheimer's disease. Science 2010;330(6012):1774.
3. Tarasoff-Conway JM, Carare RO, Osorio RS, et al. Clearance systems in the brain-implications for Alzheimer disease. Nat Rev Neurol 2015;11(8):457–470. [Published correction appears in Nat Rev Neurol 2016;12(4):248.]
4. Solár P, Zamani A, Kubíčková L, Dubový P, Joukal M. Choroid plexus and the blood-cerebrospinal fluid barrier in disease. Fluids Barriers CNS 2020;17(1):35.
5. Ghersi-Egea JF, Strazielle N, Catala M, Silva-Vargas V, Doetsch F, Engelhardt B. Molecular anatomy and functions of the choroidal blood-cerebrospinal fluid barrier in health and disease. Acta Neuropathol (Berl) 2018;135(3):337–361.
6. Serot JM, Béné MC, Foliguet B, Faure GC. Morphological alterations of the choroid plexus in late-onset Alzheimer's disease. Acta Neuropathol (Berl) 2000;99(2):105–108.
7. Wen GY, Wisniewski HM, Kascsak RJ. Biondi ring tangles in the choroid plexus of Alzheimer's disease and normal aging brains: a quantitative study. Brain Res 1999;832(1-2):40–46.
8. Dietrich MO, Spuch C, Antequera D, et al. Megalin mediates the transport of leptin across the blood-CSF barrier. Neurobiol Aging 2008;29(6):902–912.
9. Fishman RA. The cerebrospinal fluid production rate is reduced in dementia of the Alzheimer's type. Neurology 2002;58(12):1866; author reply 1866.
10. Bolos M, Antequera D, Aldudo J, Kristen H, Bullido MJ, Carro E. Choroid plexus implants rescue Alzheimer's disease-like pathologies by modulating amyloid-β degradation. Cell Mol Life Sci 2014;71(15):2947–2955.
11. Wolburg H, Paulus W. Choroid plexus: biology and pathology. Acta Neuropathol (Berl) 2010;119(1):75–88.
12. Kaur C, Rathnasamy G, Ling EA. The choroid plexus in healthy and diseased brain. J Neuropathol Exp Neurol 2016;75(3):198–213.
13. Oshima S, Fushimi Y, Okada T, et al. Brain MRI with quantitative susceptibility mapping: relationship to CT attenuation values. Radiology 2020;294(3):600–609.
14. Tadayon E, Pascual-Leone A, Press D, Santarnecchi E; Alzheimer's Disease Neuroimaging Initiative. Choroid plexus volume is associated with levels of CSF proteins: relevance for Alzheimer's and Parkinson's disease. Neurobiol Aging 2020;89:108–117.
15. Moon WJ, Lim C, Ha IH, et al. Hippocampal blood-brain barrier permeability is related to the APOE4 mutation status of elderly individuals without dementia. J Cereb Blood Flow Metab 2021;41(6):1351–1361.
16. Moon Y, Lim C, Kim Y, Moon WJ. Sex-related differences in regional blood-brain barrier integrity in non-demented elderly subjects. Int J Mol Sci 2021;22(6):2860.
17. McKhann G, Drachman D, Folstein M, Katzman R, Price D, Stadlan EM. Clinical diagnosis of Alzheimer's disease: report of the NINCDS-ADRDA Work Group under the auspices of Department of Health and Human Services Task Force on Alzheimer's Disease. Neurology 1984;34(7):939–944.
18. McKhann GM, Knopman DS, Chertkow H, et al. The diagnosis of dementia due to Alzheimer's disease: recommendations from the National Institute on Aging-Alzheimer's Association workgroups on diagnostic guidelines for Alzheimer's disease. Alzheimers Dement 2011;7(3):263–269.
19. Petersen RC, Smith GE, Waring SC, Ivnik RJ, Tangalos EG, Kokmen E. Mild cognitive impairment: clinical characterization and outcome. Arch Neurol 1999;56(3):303–308.
20. Jessen F, Amariglio RE, Buckley RF, et al. The characterisation of subjective cognitive decline. Lancet Neurol 2020;19(3):271–278.
21. Edmonds EC, McDonald CR, Marshall A, et al. Early versus late MCI: improved MCI staging using a neuropsychological approach. Alzheimers Dement 2019;15(5):699–708.
22. Kang Y, Na D, Hahn S. Seoul neuropsychological screening battery. Incheon, Korea: Human Brain Research & Consulting Co, 2003.
23. Park M, Moon WJ, Moon Y, Choi JW, Han SH, Wang Y. Region-specific susceptibility change in cognitively impaired patients with diabetes mellitus. PLoS One 2018;13(10):e0205797.
24. Thrippleton MJ, Backes WH, Sourbron S, et al. Quantifying blood-brain barrier leakage in small vessel disease: review and consensus recommendations. Alzheimers Dement 2019;15(6):840–858.
25. Cho Y, Seong JK, Jeong Y, Shin SY; Alzheimer's Disease Neuroimaging Initiative. Individual subject classification for Alzheimer's disease based on incremental learning using a spatial frequency representation of cortical thickness data. Neuroimage 2012;59(3):2217–2230.
26. Lee JS, Kim C, Shin JH, et al. Machine learning-based individual assessment of cortical atrophy pattern in Alzheimer's disease spectrum: development of the classifier and longitudinal evaluation. Sci Rep 2018;8(1):4161.
27. Lee J, Lee JY, Oh SW, et al. Evaluation of reproducibility of brain volumetry between commercial software, Inbrain and established research purpose method, FreeSurfer. J Clin Neurol 2021;17(2):307–316.

28. Heye AK, Thrippleton MJ, Armitage PA, et al. Tracer kinetic modelling for DCE-MRI quantification of subtle blood-brain barrier permeability. Neuroimage 2016;125:446–455.
29. Li W, Wu B, Liu C. Quantitative susceptibility mapping of human brain reflects spatial variation in tissue composition. Neuroimage 2011;55(4):1645–1656.
30. Yoon J, Gong E, Chatnuntawech I, et al. Quantitative susceptibility mapping using deep neural network: QSMnet. Neuroimage 2018;179:199–206.
31. Jung W, Yoon J, Ji S, et al. Exploring linearity of deep neural network trained QSM: QSMnet+. Neuroimage 2020;211:116619.
32. Straub S, Schneider TM, Emmerich J, et al. Suitable reference tissues for quantitative susceptibility mapping of the brain. Magn Reson Med 2017;78(1):204–214.
33. Santos CR, Duarte AC, Quintela T, et al. The choroid plexus as a sex hormone target: functional implications. Front Neuroendocrinol 2017;44:103–121.
34. Ricigliano VAG, Morena E, Colombi A, et al. Choroid plexus enlargement in inflammatory multiple sclerosis: 3.0-T MRI and translocator protein PET evaluation. Radiology 2021;301(1):166–177.
35. Schmid Daners M, Knobloch V, Soellinger M, et al. Age-specific characteristics and coupling of cerebral arterial inflow and cerebrospinal fluid dynamics. PLoS One 2012;7(5):e37502.
36. Schiffer E, Van Gessel E, Gamulin Z. Influence of sex on cerebrospinal fluid density in adults. Br J Anaesth 1999;83(6):943–944.
37. González-Marrero I, Castañeyra-Ruiz L, González-Toledo J, et al. High blood pressure effects on the brain barriers and choroid plexus secretion. Neurosci Med 2012;3(1):60–64.
38. Achariyar TM, Li B, Peng W, et al. Glymphatic distribution of CSF-derived apoE into brain is isoform specific and suppressed during sleep deprivation. Mol Neurodegener 2016;11(1):74 [Published correction appears in Mol Neurodegener 2017;12(1):3.]
39. Bouzerar R, Chaarani B, Gondry-Jouet C, Zmudka J, Balédent O. Measurement of choroid plexus perfusion using dynamic susceptibility MR imaging: capillary permeability and age-related changes. Neuroradiology 2013;55(12):1447–1454.
40. Szmydynger-Chodobska J, Chodobski A, Johanson CE. Postnatal developmental changes in blood flow to choroid plexuses and cerebral cortex of the rat. Am J Physiol 1994;266(5 Pt 2):R1488–R1492.
41. Stopa EG, Tanis KQ, Miller MC, et al. Comparative transcriptomics of choroid plexus in Alzheimer's disease, frontotemporal dementia and Huntington's disease: implications for CSF homeostasis. Fluids Barriers CNS 2018;15(1):18.
42. Yalcin A, Ceylan M, Bayraktutan OF, Sonkaya AR, Yuce I. Age and gender related prevalence of intracranial calcifications in CT imaging; data from 12,000 healthy subjects. J Chem Neuroanat 2016;78:20–24.
43. Ikonomovic MD, Abrahamson EE, Price JC, Mathis CA, Klunk WE. [F-18] AV-1451 positron emission tomography retention in choroid plexus: more than "off-target" binding. Ann Neurol 2016;80(2):307–308.